Al-Rafidain Journal of Engineering Sciences

Journal homepage https://rjes.iq/index.php/rjes

ISSN 3005-3153 (Online)

Experimental Investigation on the Ultimate Strength of Corroded Composite Concrete Beams Strengthened with NSM GFRP Bars

Aws Dh. Hammadi[1], Ali H.Aziz[2]

[1,2] Department of Civil Engineering, College of Engineering, Mustansiriyah University, 10064 Baghdad, Iraq

ARTICLE INFO

Article history:
Received 26 May 2025
Revised 26 May 2025
Accepted 15 June 2025
Available online 22 June 2025

Keywords:
Corrosion
Composite Concrete Beams
Near-Surface Mounted (NSM) Technique
GFRP Bars
Self-Compacting Concrete (SCC)

ABSTRACT

This study examined the impact of corrosion on the ultimate strength of composite concrete beams and assessed the effectiveness of Glass Fiber Reinforced Polymer (GFRP) bars applied using the Near-Surface Mounted (NSM) technique. Five composite beams were cast and tested, each comprising a self-compacting concrete (SCC) web and a normal-strength concrete (NC) slab connected by vertical steel links. The primary variables were corrosion level and the location of GFRP strengthening. One specimen was used as a control, while the remaining four were exposed to either partial corrosion (50 mm into the slab) or full-depth corrosion across the entire cross-section. GFRP bars were applied through the NSM technique at two positions: within the slab region and in the tensile zone of the beam. Experimental results showed that corrosion significantly reduced load-carrying capacity, especially in fully corroded specimens, which failed earlier. However, NSM-GFRP bars enhanced the structural execution of corroded beams. Strengthening applied in the tensile zone yielded greater recovery in strength compared to slab-region application. The findings highlighted the importance of both corrosion severity and reinforcement placement in determining structural behavior. The study offered practical guidance for strengthening deteriorated composite beams using NSM GFRP systems.

1. Introduction

Composite materials have become increasingly important across multiple engineering disciplines, such as civil, mechanical, and aeronautical engineering, due to their superior performance compared to traditional materials. They provide benefits such as a superior ratio of strength to weight, increased stiffness, corrosion and wear resistance, higher thermal properties, and prolonged fatigue life [1]. Composite structures have seen widespread use in both industrial and civil construction in recent years. By combining steel and concrete into a fully integrated system, composite structures effectively overcome many of the limitations associated with using either material alone, offering enhanced structural performance and efficiency[2]. Steel-concrete composite beams have grown in popularity for bridge building in recent years. For several years due to their efficient structural performance and durability[3]. Highway bridges and other modern structures frequently use composite steel-concrete construction owing to its structural efficacy. These systems provide an elevated span-to-depth ratio, enhanced stiffness, and diminished deflections in comparison to conventional steel or concrete beam structures. This makes them particularly suitable for applications such as highway bridges, where long spans and high load demands are common [4]. Clause 17.5 of ACI

Corresponding author E-mail address: aws.dhari@uomustansiriyah.edu.iq
https://doi.org/10.61268/95mhet70

Building Code 318 (ACI 1999) delineates the design and detailing specifications for horizontal shear transmission in composite concrete beams. According to the code, a composite member or portions of it can be employed to withstand moments and shear without distinguishing between shored and unshored elements for strength assessments.

Furthermore, for deflection analysis, the code allows composite members constructed with temporary supports (shored construction) to be treated as monolithically cast elements[5]. Composite construction offers a cost-effective method for integrating precast and cast-in-place concrete to maintain the integrity of the structure as well as the efficiency of rigid structures. Composite beams are typically smaller, shallower, and lighter, contributing to overall material and construction cost savings. For such beams to function as a unified structural element, the cast-in-place slab with the precast girder needs to cooperate. This monolithic behavior depends on the effective transfer of the interface's horizontal shear, which is affected by variables including the surface irregularity of the precast beam, the quantity of transverse reinforcement intersecting the junction, and the concrete's compressive strength [6]. The corrosion of reinforcement steel is a principal factor in the degradation of reinforced concrete (RC) constructions. The corrosion process converts steel into rust, leading to two primary consequences: (1) a decrease in the reinforcing bars' cross-sectional area and (2) a volumetric expansion that induces internal tensile stresses in the surrounding concrete, potentially leading to cracking, spalling of the concrete cover, and degradation of the bond between the steel and the concrete [7]. Steel reinforcement corrosion, primarily initiated by chloride infiltration and/or carbonation in hostile settings, is the predominant kind of steel degradation in concrete constructions. Chloride-induced and carbonation-induced corrosion differ significantly, particularly in their effects on cross-sectional area loss. Damage from corrosion in constructions Reinforced concrete (RC) is often characterized by a reduction in the cross-sectional area of the steel, leading to a deterioration of mechanical properties such as yield strength, ultimate strength, and ductility, ultimately culminating in premature structural failure [8] The corrosion of steel reinforcement is a critical component in the deterioration of reinforced concrete (RC) structures, severely undermining the safety and longevity of civil infrastructure [9].

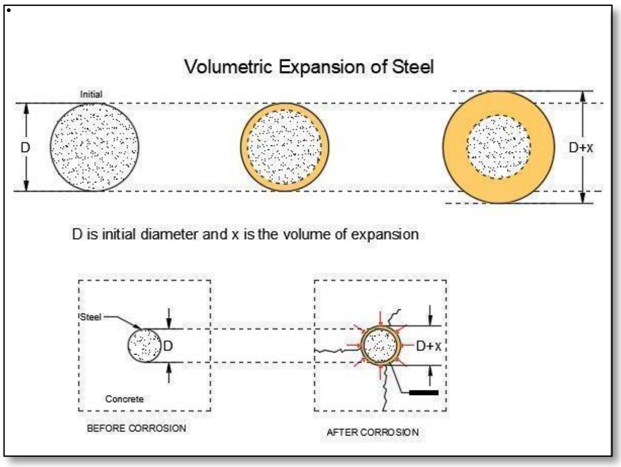

Figure 1 Volumetric expansion of steel[10]

Steel reinforcement corrosion causes progressive damage to concrete, including cracking, delamination, and delamination of the concrete surface. This deterioration results in a reduction in the structural member's strength, whether flexural, shear, or otherwise, as well as a significant loss in ductility[11]. Various types of concrete have been extensively used in construction and water infrastructure projects due to their diverse strengths, shapes, and overall reliable performance. However, in harsh environments such as marine conditions, de-icing salt exposure, saline-alkali soils, and brine-contaminated industrial zones, reinforced concrete is highly vulnerable to corrosion, posing a significant threat to the longevity and operational lifespan of concrete buildings [12]. In extreme conditions, the degradation of steel reinforcement in reinforced concrete (RC) constructions can result in a substantial decrease in load-bearing capacity. While this does not always result in collapse, particularly in above-ground structures where deterioration may be visually detected and addressed through maintenance or repairs, it poses a more serious risk in underground or inaccessible structural components. In such cases, undetected corrosion can progress unchecked, compromising structural integrity. Additionally, corrosion may induce brittle fracture in the reinforcement, increasing the likelihood of failure under fatigue loading conditions[13]. Corrosion can significantly influence the strength of the concrete-steel reinforcing link. First, the growth of corrosion products may increase radial stresses at the interface between steel and concrete, enhancing friction and temporarily improving bond strength. However, as corrosion progresses, it leads to longitudinal cracking and weakens the concrete's ability to resist bursting forces around the reinforcement. Some studies suggest that, in early stages, a tightly adherent rust layer might actually improve bond strength, though this effect diminishes with continued deterioration [14]. In fact, corrosion reduces the structural strength of reinforced concrete (RC) constructions and is primarily enhanced by reducing the diameter of both longitudinal reinforcing bars and stirrups[15]. Corrosion results possess greater amounts than the original steel, inducing tensile strains in the adjacent concrete and resulting in the cracking of the concrete cover. As a result, the flexural strength of corroded reinforced concrete structures diminishes due to the decrease in the steel cross-sectional area and the degradation of the link between the reinforcement and the adjacent concrete.[16]. In recent decades, substantial research has concentrated on the flexural performance of concrete beams reinforced with fiber-reinforced polymer (FRP) bars. Two principal failure modes have been identified. The first is a tension-controlled failure, marked by the sudden rupture of FRP bars, which is often catastrophic and occurs with minimal warning due to the low ductility of FRP materials. The second is a compression-controlled failure, which is generally more desirable, as it allows the member to demonstrate inelastic behavior via concrete failure prior to FRP rupture, providing a more gradual failure response[17]. Comprehensive studies conducted over recent decades have recognized fiber-reinforced polymer (FRP) reinforcements as a feasible substitute for conventional steel bars. FRP bars provide exceptional corrosion resistance, an advantageous strength-to-weight ratio, superior fatigue performance, a reduced elastic modulus relative to steel, and a linear stress-strain relationship. Available commercial varieties of FRP encompass glass (GFRP), carbon (CFRP), aramid (AFRP), and basalt (BFRP). Among these, GFRP bars are the most frequently utilized in practice owing to their cost-effectiveness and appropriate mechanical qualities[18]. Fiber-reinforced polymer (FRP) composites are increasingly considered alternatives to steel rebars and tendons in certain concrete structural members. Current research primarily focuses on evaluating the strength and durability of both the FRP materials themselves and the concrete elements reinforced with these composites[19]. Recent studies indicate that employing high-strength concrete can mitigate crack widths in beams reinforced with FRP bars. This is mostly due to the enhancement of bond strength between FRP bars and the adjacent concrete when compressive strength rises. ACI 440.1R-15 states that the bond strength at the contact is roughly proportional to the square root of the concrete's compressive strength[20].

NSM FRP bars have demonstrated efficacy in fortifying reinforced concrete (RC) beams by augmenting bond capacity and offering protection against external damage[21]. The strengthening of NSM has emerged as a prevalent method for augmenting the flexural capacity of concrete elements, principally owing to its reduced susceptibility to debonding failure [22]. NSM-FRP is a promising technique for strengthening both existing and new structures, offering advantages over externally bonded reinforcement (EBR), particularly through improved strain distribution that allows for greater utilization of the material's capacity[23]. Structural strengthening is often required due to changes in design codes, seismic retrofitting needs, environmental deterioration, or increased service loads resulting from changes in the structure's use[24].

2. Experimental work

2.1. Experimental program

The experimental work involved the casting and testing of five composite concrete beam specimens. Each specimen consisted of a reinforced (SCC) web combined with (NC) slab acting as the flange. Vertical steel links served as shear connectors between the two layers. The variables considered in the study included the presence of corrosion and the application of GFRP strengthening. The steel grade, concrete grade of the slab, and both transverse and longitudinal reinforcement were consistent across all specimens. The coding of the beam specimens is presented in Table 1.

.

Table 1 Beam Specimens Coding and Details

Beam Coding	**Web**		**Slab (Flange)**	
	Corrosion	**Strengthening**	**Corrosion**	**Strengthening**
B 1	None	None	None	None
B 2	None	None	Corroded	None
B 4	Corroded	None	Corroded	None
B 3	None	None	Corroded	Strengthened
B 5	Corroded	Strengthened	Corroded	None

2.2. Beam Specimen Description

As previously noted, the experimental program involved the fabrication and testing of five reinforced concrete composite beam specimens, each with specific geometric properties. The beams consisted of two distinct parts joined at a construction interface: a bottom web (250 mm × 150 mm) and a top slab (450 mm × 50 mm), forming a T-shaped cross-section. The total beam depth, slab width, and slab thickness were 300 mm, 450 mm, and 50 mm, respectively. Each beam measured 1600 mm in overall length, with a clear span of 1500 mm between supports. The webs were cast using SCC with an approximate compressive strength of 50 MPa, while the slabs were cast with NC of about 25 MPa compressive strength. Web reinforcement included three ϕ10 mm longitudinal bars at the bottom and two ϕ6 mm bars near the top to support the stirrups. Shear reinforcement consisted of ϕ6 mm bars spaced at 100 mm intervals. The slab was reinforced with a single bottom layer of bars in both directions, maintaining a 25 mm concrete cover. Longitudinal slab reinforcement comprised four ϕ6 mm deformed bars, while transverse reinforcement included ϕ6 mm bars spaced at 100 mm along the slab's length. The stirrups were classified into two types: extended stirrups acting as shear connectors and non-extended stirrups confined to the web. Figure 2 and Figure 3 illustrate the geometry, applied load, and reinforcement.

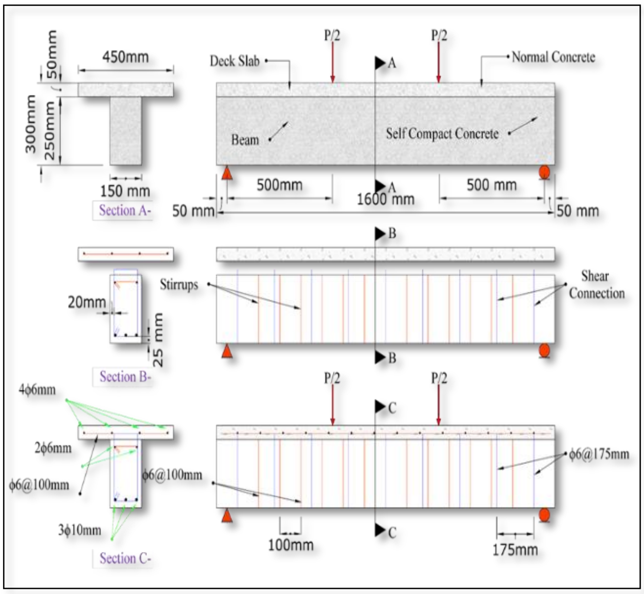

Figure 2 Beam specimens

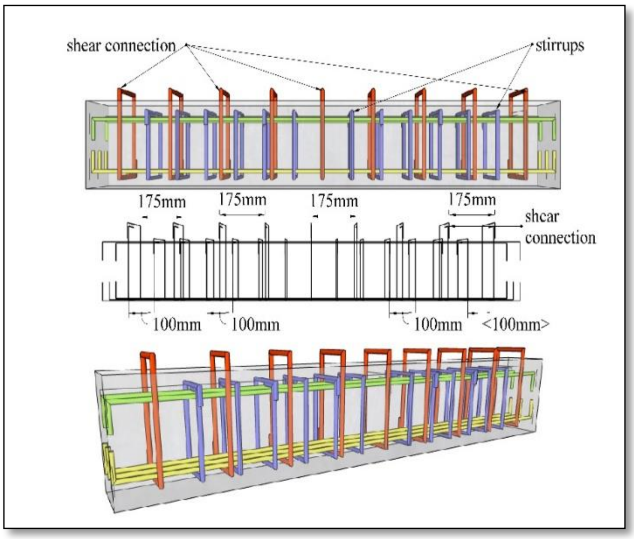

Figure 3 Beam reinforcement

3. Beam and Control Specimens Cast

All necessary raw materials and equipment were systematically organized to facilitate the on-site casting of composite beam specimens and control samples (cylinders, cubes, and prisms) for evaluating the mechanical properties of the hardened concrete. Steel cages for the beams and reinforcement layers for the deck slabs were carefully assembled and positioned prior to casting. The concrete components were mixed according to the specified mix design, transported, and placed into molds. Following casting, all specimens were demolded after initial setting and cured in water for 28 days to enhance hydration and minimize moisture loss, ensuring optimal long-term strength. The composite beams were cast in two stages: first, the lower section (web) was poured and cured; after several days, the upper section (slab) was cast, completing the composite configuration. This sequential casting approach is illustrated in Figure 4

Figure 4 Beam Specimens Cast

4. Accelerated (Artificial) Corrosion Mechanism

An electrochemical method is used to expedite the degradation of both longitudinal and transverse reinforcement in composite beams, which indirectly facilitates the deterioration of the two concretes used (NC) and (SCC). Two levels of corrosion were administered to the tested composite beams. The first phase entails revealing the upper section of the beam (flange), which encompasses the deck slab level, characterized by a thickness of just (50 mm). The subsequent phase is subjecting the whole beam to corrosion at a height of (300 mm). A consistent corrosion rate was established for both levels, resulting in an estimated (30%) reduction in the mass of the steel bars utilized to fabricate the tested beam specimens for this study. Three concrete containers (tanks) were used to do the accelerated (artificial) corrosion process. The dimension of the first tank was (2m x 2mm), the second tank was (2.2m x 1.4m), and the third tank was (2.6m x 1.8m). Four samples were allocated to the first tank, and two samples were designated for the second tank to initiate the corrosion process at the upper section (flange) of the tested composite beams, leading to corrosion with (50mm) depth from the surface of the beam's deck slab. The third tank included six samples of the tested composite beams, which were designated for prolonged corrosion exposure. The longitudinal and transverse reinforcement bars were exposed to an electric current generated by using an external direct current power source, thereby accelerating the corrosion process. The beam specimens were positioned into the tanks with hardwood bases of (50 mm) thickness, facilitating a conducive, humid environment while permitting the submerged bottom surface to experience corrosion. The beam specimens were immersed in (10%) NaCl saline solution for (24 hours) before initiating the electrochemical corrosion process. The electrical connection method used longitudinal rebar and ring bars as anodes inked to the positive terminal of the direct current (DC) source via wires for integration, as shown in Figure 5. The negative terminal was externally connected using (4mm) thick iron components, serving as negative electrodes. Each segment measured 750 mm in length and 100 mm in breadth. A portion was positioned next to each specimen immersed in the tank and interconnected in a series configuration. A direct current (DC) source was used to facilitate this process, applying a current density of 1.5 mA/cm² to the surface area of the reinforcement employed in the composite beams. The duration required for each controlled parameter varied, as seen in Figures 6 and 7. It may be noted that the current study used Faraday's law as a conceptual framework to ascertain the time necessary for deterioration due to the corrosion process, using the relevant equation (1), [25], [26]

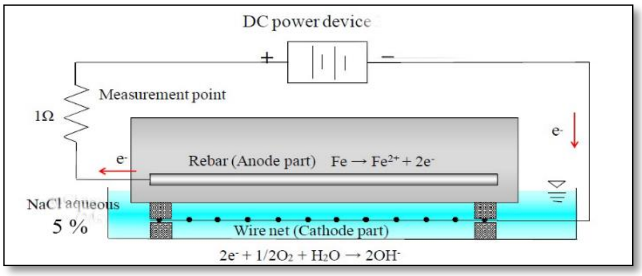

Figure 5 Accelerated corrosion set-up [28]

Figure 6 Phases of the corrosion process for first-level specimens

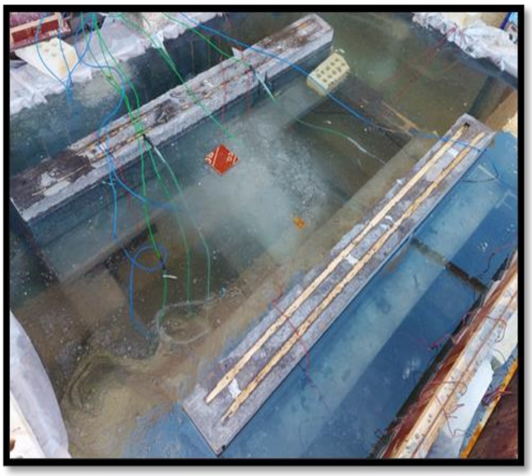

Figure 7 Phases of the corrosion process for second-level specimens

$$M=(I\ T\ S\ a / n\ F) \quad \ldots\ (1)$$

Where:

M = Mass losses (g)

I = Current density (A/cm2)

T = Corrosion time (seconds)

S = The surface area of corroded stirrups (cm^2)

a = The weight of the atomic metal (56 g /mol for Iron Fe+2)

n = numbers of iron electrons transmitted through the corrosion process (n = 2 for Fe+2)

F = Faraday's constant (96.500 C/mol)

5. NSM Technique using GFRP Bars

In this study, the NSM technique with GFRP bars was employed to strengthen both the top (flange) and bottom (web) regions of corroded composite beam specimens, aiming to improve their structural performance. A critical aspect of using FRP materials for strengthening is ensuring proper adhesion between the FRP and the concrete substrate. To achieve this, the beam surfaces were thoroughly prepared: grooves formed during casting were carefully cleaned using a soft brush, and residual dust was removed with an air blower. A high-performance epoxy adhesive, Sikadur-31 CF, was used to bond the GFRP bars. The epoxy's two components (A and B) were mixed at the manufacturer's recommended weight ratio of 1:2. The mixed epoxy was applied into the grooves, followed by the placement of the GFRP bars. The grooves were then sealed with an additional epoxy layer, as illustrated in Figure 7. The assembly was left to cure for 10 days in accordance with the manufacturer's guidelines.

Figure 8 Implementing the NSM technology on corroded beams

6. Test Procedure

The beam specimens were tested under incremental monotonic load using load control criteria. A two-point loading test was performed on all tested beam specimens. A force was exerted on steel-bearing plates to transfer the weight to the concrete beams, averting local failure, Figure 9. To observe the progression of cracks, the beam specimens were coated (painted) with white color paint. Consequently, the fissures were apparent during the experimental test of the beam specimens. Two linear variable differential transformers (LVDTs) were positioned on the bottom face of the tested beams for bending testing; the first one was fixed at the mid-point of the tested beam, and the other was fixed under the location of one of the two-point loading. The beam specimens were tested using an electric hydraulic machine with a maximum capability of (500 kN). Loads were incrementally applied to the tested beams until the failure threshold was attained. All measured and observed deflections for each beam specimen were documented with a data logger. Marks were applied to the cracks that emerged during the test utilizing coloring pens, and the width of the cracks for each model was quantified using a digital microscope, as illustrated in Figure 10.

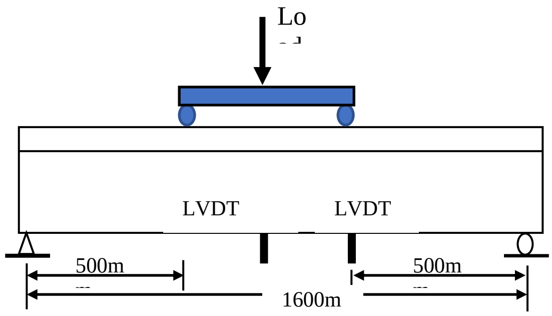

Figure 9 Beam specimens set-up

Figure 10 Beam specimen's test

7. Disassembling the tested beams post-evaluation

After the compilation of the beam specimen tests, some samples were extracted from those subjected to corrosion to analyze the impact of corrosion on concrete composition and reinforcing steel bars (longitudinal and lateral), particularly concerning the shear connections of the composite beams, Figure 11. Various samples of corroded reinforcing steel bars were collected for laboratory analysis, Figure 12; the bars were cleaned by removing rust and mortar residue around their surfaces by brushing. The test findings of the corroded steel bars were juxtaposed with those of the non-corroded steel bars, and the extent of loss in the reinforcement steel attributable to corrosion was quantified in Table 3.

Figure 11 Corrosion-prone models were disassembled after testing.

Figure 12 Corroded and non-corroded steel bars tensile test

Table 3 Tensile Test Results of The Corroded Steel Bars

Diameter	Test results before the corrosion process		Test results after the first level, 50 mm depth of corrosion		Test results after the second level, 300 mm depth of corrosion	
	fy	*fu*	*fy*	*fu*	*fy*	*fu*
6mm	550	600	354	388	350	382
10mm	465	661	457	650	370	526

8. Beam Specimens Tests Results and discussion

8.1 Effect of corrosion on ultimate load capacity

Following corrosion exposure and strengthening interventions, five composite beam specimens (B1–B5) were tested under direct loading for the ultimate load capacity; the test results are plotted and illustrated in Figure 12. The reference specimen (B1) exhibited the highest ultimate load and served as a benchmark for performance comparison. Specimen B2, subjected to partial corrosion without strengthening, showed a 9% reduction in ultimate capacity compared to B1, while B3, strengthened using GFRP bars embedded in the slab region (flange) via the NSM technique after corrosion, experienced a 14% reduction. Although strengthened, B3’s performance was still affected, indicating that slab-only reinforcement may not fully recover the lost capacity. In contrast, specimen B4, fully corroded and left unstrengthened, showed a 29% reduction, highlighting the severe effect of corrosion on load-bearing capacity. Notably, B5 strengthened with GFRP bars in the tensile zone (web demonstrated improved performance over B4, confirming the higher effectiveness of flexural zone reinforcement in restoring structural capacity. These results underscore the detrimental impact of corrosion on composite concrete beams and demonstrate that the location of GFRP reinforcement plays a crucial role in recovery. Strengthening in the tension zone (web) proved more effective than in the slab region alone, suggesting that targeted flexural reinforcement is key for post-corrosion structural rehabilitation.

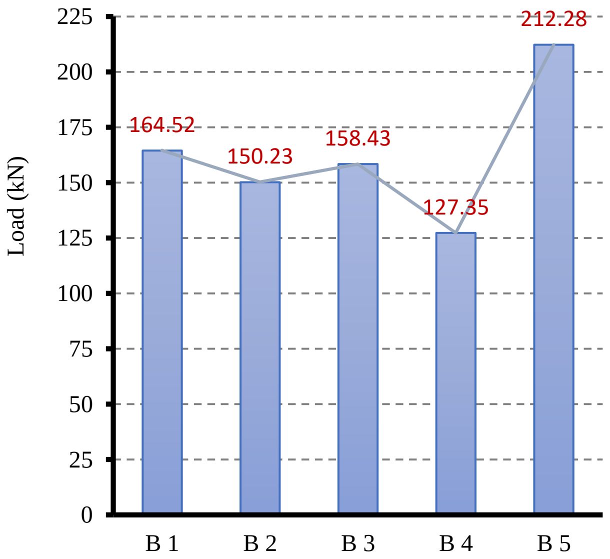

Figure 13 Effect of Corrosion on (Pu) of tested beams

8.2 Effect of Corrosion on the Deflection

The experimental tests performed on all beam specimens pertinent to this paper yielded the necessary data for the preparation of various graphs, which include the determination of vertical displacements (vertical deflection). The findings indicate that the corrosion had a more pronounced impact on the vertical deflection of fully corroded samples compared to partly corroded beam specimens, which included deck slab with a depth of 50 mm. as demonstrated in Figures 13,

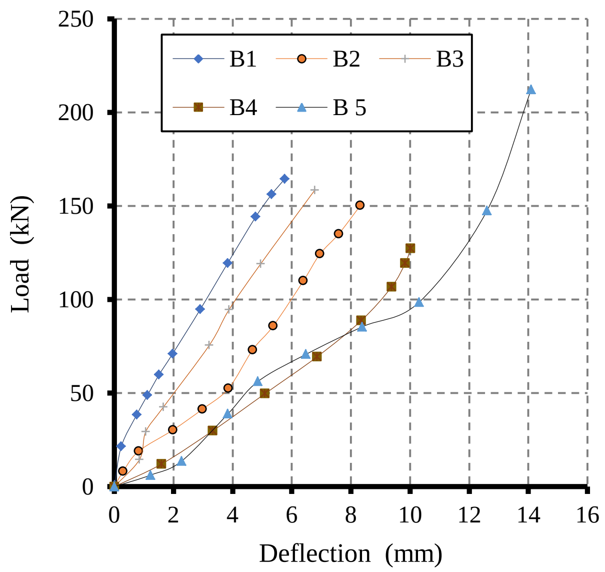

Figure 14 Mid-Span Load-Deflection Curves of Beam Specimen

8.3 Effect of Strengthening

As mentioned before, the current research includes a study of the impact of using GFRP bars as NSM on the structural performance of the tested beams. The test results show a noticeable enhancement in ultimate capacity for all strengthened beam specimens. For the tested beams of group-1, (B-3), and (B-5), the ultimate capacity was increased by about (5%) and (67%) respectively, in comparison with the corresponding corroded non-strengthened beam specimens. The corroded beam specimens that were strengthened by GFRP bars as NSM at the extreme bottom fibers (at the web) (B-5) exhibited more enhancement compared to those strengthened by GFRP bars as NSM at the bottom fibers of the deck slab (flange), (B-3); the utilization of GFRP bars at the extreme bottom fibers leads to generate additional resisting components which leads to a significant increase in ultimate load relative to the reference beams.

Regarding the load-deflection response, Figure 13 illustrates the load-deflection curves for beams reinforced with lower NSM GFRP bars (B5), measuring 1500 mm long. The data indicates that the beam reinforced with lower NSM GFRP bars exhibited superior load capacities compared to the beam specimens that strengthened at the bottom face of the deck slab (B3) with NSM GFRP bars, measuring 1500 mm long. Notably, these beams showed significantly enhanced load-bearing capacity relative to the reference beams.

9. Summary and Conclusions

This study involved testing five composite concrete-concrete beam specimens to assess the influence of corrosion and strengthening using the NSM technique with GFRP bars on the structural behavior of the beams, including ultimate load capacity mid-span deflection. The results clearly demonstrated that corrosion had a detrimental effect on the ultimate load capacity of the composite beams, significantly reducing their structural efficiency and integrity.

However, the application of GFRP bars using the NSM technique effectively restored and enhanced the load-bearing capacity of the corroded beams, particularly when applied in the tension zone. Key findings and recommendations are summarized as follows:

- The study revealed that beam specimens subjected to full corrosion experienced earlier failure and a significantly greater reduction in ultimate load capacity compared to those with partial corrosion and reference specimens.
- The study demonstrated that corrosion significantly reduces the compressive strength of reinforced concrete beams, leading to complex deterioration of the concrete matrix and compromising the structural integrity.
- For the fully corroded beam specimens, the findings revealed that using GFRP bars with the NSM technique significantly improved the ultimate load capacity, particularly when applied at the extreme bottom fibers (tension zone) of the beams.

References

[1] E. Madenci, Y. O. Özkılıç, and L. Gemi, “Experimental and theoretical investigation on flexure performance of pultruded GFRP composite beams with damage analyses,” *Compos Struct*, vol. 242, Jun. 2020, doi: 10.1016/j.compstruct.2020.112162.

[2] Y. H. Wang, J. G. Nie, and C. S. Cai, “Numerical modeling on concrete structures and steel-concrete composite frame structures,” *Compos B Eng*, vol. 51, pp. 58–67, Aug. 2013, doi: 10.1016/j.compositesb.2013.02.035.

[3] J. Xu, H. Sun, W. Chen, and X. Guo, “Experiment-based fatigue behaviors and damage detection study of headed shear studs in steel-concrete composite beams,” *Applied Sciences (Switzerland)*, vol. 11, no. 18, Sep. 2021, doi: 10.3390/app11188297.

[4] E. L. Tan and B. Uy, “Experimental study on curved composite beams subjected to combined flexure and torsion,” *J Constr Steel Res*, vol. 65, no. 8–9, pp. 1855–1863, Aug. 2009, doi: 10.1016/j.jcsr.2009.04.015.

[5] A. K. Patnaik, “Behavior of Composite Concrete Beams with Smooth Interface,” *Journal of Structural Engineering*, vol. 127, no. 4, pp. 359–366, Apr. 2001, doi: 10.1061/(ASCE)0733-9445(2001)127:4(359).

[6] R. E. Loov D Phil, P. Eng, and A. K. Patnaik, “Horizontal Shear Strength of Composite Concrete Beams With a Rough Interface.”

[7] K. Zandi and K. Lundgren, “Analysis of Mechanical Behavior of Corroded Reinforced Concrete Structures,” 2011. [Online]. Available: https://www.researchgate.net/publication/259968652

[8] G. G. Triantafyllou, T. C. Rousakis, and A. I. Karabinis, “Corroded RC beams patch repaired and strengthened in flexure with fiber-reinforced polymer laminates,” *Compos B Eng*, vol. 112, pp. 125–136, Mar. 2017, doi: 10.1016/j.compositesb.2016.12.032.

[9] A. Zheng, Z. Liu, F. Li, and S. Li, “Experimental investigation of corrosion-damaged RC beams strengthened in flexure with FRP grid-reinforced ECC matrix composites,” *Eng Struct*, vol. 244, Oct. 2021, doi: 10.1016/j.engstruct.2021.112779.

[10] S. Rajappa, V. Shree, and B. Gowda, “FRP STRENGTHENING OF RC BEAMS WITH CORRODED STEEL REINFORCEMENT Structural Engineering and Building Technology.”

[11] A. Tarighat and B. Zehtab, “Structural Reliability of Reinforced Concrete Beams/Columns Under Simultaneous Static Loads and Steel Reinforcement Corrosion,” *Arab J Sci Eng*, vol. 41, no. 10, pp. 3945–3958, Oct. 2016, doi: 10.1007/s13369-016-2033-6.

[12] H. Zhu, J. Liang, J. Xu, M. Bo, J. Li, and B. Tang, “Research on anti-chloride ion penetration property of crumb rubber concrete at different ambient temperatures,” *Constr Build Mater*, vol. 189, pp. 42–53, Nov. 2018, doi: 10.1016/j.conbuildmat.2018.08.193.

[13] W. Yi and F. Tang, “Fatigue Behavior of Reinforced Concrete Beams with Corroded Steel Reinforcement.” [Online]. Available: https://www.researchgate.net/publication/266384685

[14] A. N. Patil, B. G. Birajdar, and H. K. Erande, “Study of Influence of Corrosion and Cracking on Bond Behavior of Reinforced Concrete Member Journal of Structural Engineering and Management Study of Influence of Corrosion and Cracking on Bond Behavior of Reinforced Concrete Member,” pp. 58–67, 2017, [Online]. Available: www.stmjournals.com

[15] A. Bossio *et al.*, “Corrosion effects on seismic capacity of reinforced concrete structures,” *Corrosion Reviews*, vol. 37, no. 1, pp. 45–56, Feb. 2019, doi: 10.1515/corrrev-2018-0044.

[16] G. Malumbela, M. Alexander, and P. Moyo, “Variation of steel loss and its effect on the ultimate flexural capacity of RC beams corroded and repaired under load,” *Constr Build Mater*, vol. 24, no. 6, pp. 1051–1059, Jun. 2010, doi: 10.1016/j.conbuildmat.2009.11.012.

[17] H. L. Dong, W. Zhou, and Z. Wang, “Flexural performance of concrete beams reinforced with FRP bars grouted in corrugated sleeves,” *Compos Struct*, vol. 215, pp. 49–59, May 2019, doi: 10.1016/j.compstruct.2019.02.052.

[18] W. Xue, F. Peng, and Q. Zheng, “Design Equations for Flexural Capacity of Concrete Beams Reinforced with Glass Fiber–Reinforced Polymer Bars,” *Journal of Composites for Construction*, vol.

20, no. 3, Jun. 2016, doi: 10.1061/(ASCE)cc.1943-5614.0000630.

[19] B. Antonio Nanni, "FLEXURAL BEHAVIOR AND DESIGN OF RC MEMBERS USING FRP REINFORCEMENT."

[20] H. L. Dong, W. Zhou, and Z. Wang, "Flexural performance of concrete beams reinforced with FRP bars grouted in corrugated sleeves," *Compos Struct*, vol. 215, pp. 49–59, May 2019, doi: 10.1016/j.compstruct.2019.02.052.

[21] R. M. Reda, I. A. Sharaky, M. Ghanem, M. H. Seleem, and H. E. M. Sallam, "Flexural behavior of RC beams strengthened by NSM GFRP Bars having different end conditions," *Compos Struct*, vol. 147, pp. 131–142, Jul. 2016, doi: 10.1016/j.compstruct.2016.03.018.

[22] M. Chellapandian, S. S. Prakash, and A. Sharma, "Experimental investigations on hybrid strengthening of short reinforced concrete column elements under eccentric compression," *Structural Concrete*, vol. 20, no. 6, pp. 1955–1973, Dec. 2019, doi: 10.1002/suco.201800311.

[23] A. Parvin and T. S. Shah, "Fiber reinforced polymer strengthening of structures by near-surface mounting method," Aug. 11, 2016, *MDPI AG*. doi: 10.3390/polym8080298.

[24] M. N. Nurbaiah, A. H. Hanizah, A. Nursafarina, and M. Nur Ashikin, "Flexural behaviour of RC beams strengthened with externally bonded (EB) FRP sheets or Near Surface Mounted (NSM) FRP rods method," in *CSSR 2010 - 2010 International Conference on Science and Social Research*, 2010, pp. 1232–1237. doi: 10.1109/CSSR.2010.5773725.

[25] Z. H. Lu, H. Li, W. Li, Y. G. Zhao, Z. Tang, and Z. Sun, "Shear behavior degradation and failure pattern of reinforced concrete beam with chloride-induced stirrup corrosion," *Advances in Structural Engineering*, vol. 22, no. 14, pp. 2998–3010, Oct. 2019, doi: 10.1177/1369433219855917.

[26] A. K. Azad, S. Ahmad, and B. H. A. Al-Gohi, "Flexural strength of corroded reinforced concrete beams," *Magazine of Concrete Research*, vol. 62, no. 6, pp. 405–414, Jun. 2010, doi: 10.1680/macr.2010.62.6.405.